Effects of Ionic Liquid [bmim][PF_6] on Absorption Spectra and Reaction Kinetics of the Duroquinone Triplet State in Acetonitrile

Guanglai Zhu,[†,‡,§] Guozhong Wu,[*,†] Maolin Sha,[†,§] Dewu Long,[†] and Side Yao[†]

Shanghai Institute of Applied Physics, Chinese Academy of Sciences, P.O. Box 800-204, Shanghai 201800, People's Republic of China, Institute of Atomic and Molecular Physics, Anhui Normal University, Wuhu 241000, People's Republic of China, and Graduate University of Chinese Academy of Sciences, Beijing 100039, People's Republic of China

Received: September 4, 2007; In Final Form: January 23, 2008

The transient absorption spectra and photoinduced electron-transfer process of duroquinone (DQ) in mixed binary solutions of ionic liquid (IL) [bmim][PF_6] and acetonitrile (MeCN) have been investigated by laser photolysis at an excitation wavelength of 355 nm. A spectral blue shift of ^{3}DQ* was observed in the IL/MeCN mixtures compared to MeCN. At lower V_{IL}(volume fraction of IL), the interaction between DQ and the solvent is dominant, and the decay rate constant (k_{obs}) of ^{3}DQ* increases steadily with the increasing of V_{IL}; to the contrary, at higher V_{IL}, the network structures due to the hydrogen bond and viscosity are dominant, and the decay rate constant decreases obviously with increasing V_{IL}. A critical point (turnover) was observed at $V_{IL} = \sim 0.30$. The dependence of the observed growth rate (k_{gr}) of the photoinduced electron-transfer (PET) products on V_{IL} is complex and shows a special change; k_{gr} first decreases with increasing V_{IL}, then increases, and finally decreases slowly with further increasing of V_{IL}. It is speculated that the PET process in the mixture can be affected by factors including the local structure and the reorganization energy of the solvent and salt and cage effects. The change of local structure of [bmim][PF_6]/MeCN is supported by following the steady-state fluorescence behavior of the mixture, in combination with the molecular dynamics simulation of the thermodynamic property. The results revealed that the degree of self-aggregation of monomeric cations ($bmim^+$) to associated forms increases with increasing V_{IL}. This is in good agreement with the laser photolysis results for the same solutions.

1. Introduction

Room-temperature ionic liquids (RTILs) have received much attention owing to their remarkable properties including low volatility, high polarity, ease of recycling, and high selectivity.[1,2] RTILs are regarded as the most suitable solvents for green chemistry, and they have been widely used as reaction media for organic synthesis, catalysis, separation process, and polymerization.[3−6] RTILs are much different from conventional polar solvents because they consist entirely of ionic species. The properties of RTILs have recently been characterized using various experimental measures (NMR, IR, Raman, etc.).[7−10] Pulse radiolysis, laser photolysis, and steady-state and time-resolved fluorescence have also been applied to study the reaction processes occurring in RTILs.[11−28] These studies mainly focused on solvent relaxation dynamics,[15−18] electron and energy transfer kinetics.[19−23] A few papers on photoinduced electron transfer by transient absorption spectroscopy in pure RTILs are noteworthy.[20−26] Effects of RTILs on transient absorption spectra and bimolecular reaction rate constants of solutes have been partly revealed. It is suggested that most of the imidazolium ionic liquids are more polar than acetonitrile but less polar than methanol.[23] As a prototype of RTILs, 1-butyl-3-methylimidazolium hexafluorophosphate, [bmim][PF_6] has been used as a medium in which some representative photochemical reactions such as photoinduced electron transfer have been previously studied in comparison with volatile organic compounds.[20−23]

Binary liquid solutions, such as IL/water and IL/organic, are frequently used in a variety of applications such as electrochemistry and organics synthesis.[27−29] Many studies on binary systems, including our previous work, have been carried out experimentally or theoretically. Although many RTILs can be dissolved in water or organic solvents, such IL/organic solutions may be not homogeneous. Some authors,[30] based on their theoretical calculations, have speculated that neat ionic liquids or their mixtures should be regarded as nanostructured solvents. According to this speculation, local structures of the IL/organic mixed solution can be tuned by varying the IL fraction. The change in local structures may have substantial effects on the reaction kinetics of transient species in photochemical processes.

In this work, we attempted to study the effects of binary [bmim][PF_6]/MeCN solutions on the spectral and kinetic behavior of transient species by laser photolysis using duroquinone (DQ) as the probe molecule and *N*,*N*,*N*′,*N*′-tetramethyl-*p*-phenylenediamine (TMPD) as an electron donor. Our results revealed that the interaction between [bmim][PF_6] and the solute can affect the absorption spectrum of the triplet excited state of DQ (^{3}DQ*) as well as the kinetics of the electron transfer between ^{3}DQ* and TMPD. For a better understanding the effect of the local structure of mixed solutions on the kinetic behavior, we carried out a steady-sate fluorescence measurement on the IL/MeCN solutions in different volume ratios. Furthermore, the thermodynamic properties of the IL/MeCN were investigated by molecular dynamics simulation. It is found that the cations

* To whom correspondence should be addressed. Tel/Fax: +86-21-59558905. E-mail: wuguozhong@sinap.ac.cn.
† Shanghai Institute of Applied Physics, Chinese Academy of Sciences.
‡ Anhui Normal University.
§ Graduate University of Chinese Academy of Sciences.

10.1021/jp077112y CCC: $40.75
Published on Web 03/11/2008

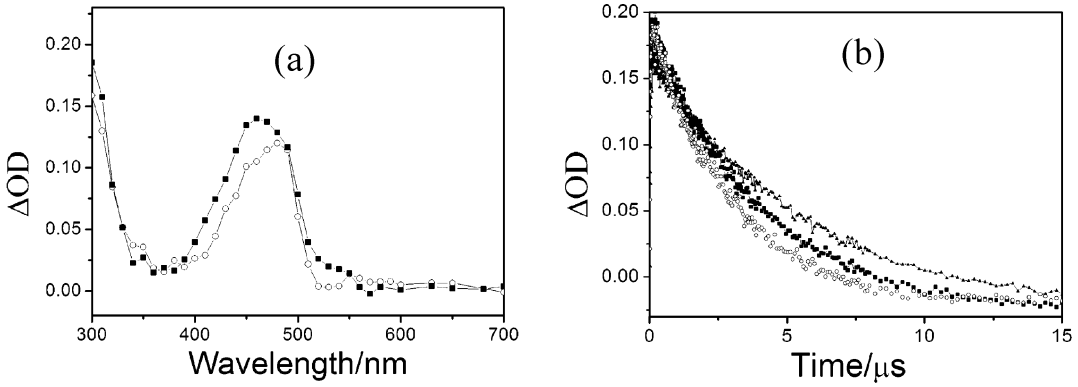

Figure 1. (a) Transient absorption spectra of ^{3}DQ* recorded at 0.1 μs after 355 nm laser excitation in a IL/MeCN solution containing 1×10^{-4} mol·dm^{-3} DQ under N_2. V_{IL}: (○) 0 and (■) 0.8. (b) Decay profiles monitored at 480 nm recorded in IL/MeCN mixed solutions in the presence of 1×10^{-4} mol·dm^{-3} DQ under N_2 purging. V_{IL}: (middle) 0, (bottom) 0.2, (top) 0.8.

of [bmim][PF_6] are present mainly in the monomeric form at lower V_{IL} but in the associated forms at higher V_{IL}.

2. Materials and Methods

All reagents were purchased from Sigma and were of the commercially available highest purity. Duroquinone (tetramethyl-*p*-benzoquinone, Me_4BQ) and TMPD were of spectral grade and used as received. The ionic liquid [bmim][PF_6] was specially treated prior to use. The [bmim][PF_6] ionic liquid was treated with activated charcoal for at least 48 h and filtered a couple of times by passing through a celite column. Then, the liquid was transferred into a clean and dry reagent bottle and kept in vacuum for 12 h at 60−65 °C to remove any volatile organic impurities and moisture. The purified ionic liquid was stored in an airproof desiccator.

Laser photolysis experiments were carried out using a Nd:YAG laser that provides 266 and 355 nm laser pulse with a duration of 5 ns and a maximum energy of 80 mJ per pulse. The probe light source was a pulsed xenon lamp. The laser and analyzing light beam passed perpendicularly through a 1 cm × 1cm quartz cell. The transmitted light signals were collected using a digital oscilloscope and then recorded by a personal computer. A detailed description of the system was described elsewhere.[31] Prior to laser irradiation, all solutions were bubbled with the appropriate gas (high-purity N_2 or O_2) for at least 20 min. All experiments were carried out at room temperature.

Fluorescence spectra were recorded in a quartz cuvette with an optical path length of 1.0 cm and at an excitation wavelength of 280 nm or 360 nm on a Hitachi F-4500 spectrofluorometer.

Some thermodynamic properties of the mixtures were computed by molecular dynamics (MD) simulation. The force field of [bmim][PF_6] used in this work is from the systematic all-atom force field developed by Lopes,[32] which is based on the optimized potentials for liquid simulation (OPLS-AA) suggested by Jorgensen et al.[33] Parameters for PF_6 were obtained from the work of Borodin.[34] A six-site model for MeCN was adopted in this work with parameters which are mainly taken from the literature,[35] except the VDW parameters of H atoms taken from OPLS-AA. The MD simulations were performed using the program Gromacs.[36] In all simulations, the bond length was constrained with LINCS. Cutoff was taken at 10 Å for Lennard-Jones interactions, and the long-range coulomb interactions were handled by PME, with a cutoff of 14 Å.

3. Results and Discussion

3.1. Transient Absorption Spectra of ^{3}DQ* in IL/MeCN Solutions. Transient absorption spectra of duroquinone triplet excited states (^{3}DQ*) have been widely studied.[37−39] Our aim is to investigate its behavior in the IL/MeCN solutions using a 355 nm laser as the excitation source. The transient absorption spectra were recorded for a series of IL/MeCN solutions containing 1×10^{-4} mol·dm^{-3} DQ. Figure 1 shows the transient absorption spectra for MeCN and IL/MeCN (volume fraction $V_{IL} = 0.8$) solutions containing DQ, obtained at 0.1 μs after the 355 nm laser pulse. It is seen that with the addition of [bmim][PF_6], a spectral blue shift of absorption band is observed, that is, a shift of λ_{max} from 480 nm in pure MeCN to 460 nm in the mixed IL/MeCN solution. In the presence of oxygen, the decay was accelerated for both solutions. The transient absorption spectrum in Figure 1 can be assigned to ^{3}DQ*. Since the absorption decays monotonically by first-order kinetics, it is concluded that the ^{3}DQ* decays mainly via self-quenching under a N_2 atmosphere. This observation is different from that of anthraquinone or benzophenone, whose excited states decay mainly via hydrogen abstraction of alkyl groups on the cations of [bmim][PF_6] under similar conditions.[27,40]

Upon excitation by a 355 nm laser, the ground state of the DQ molecule is excited to the single excited state ^{1}DQ*, and then, ^{3}DQ* is formed through intersystem crossing (ISC) (eq 1). In a N_2-saturated solution, ^{3}DQ* is self-quenched by the ground-state molecule (eq 2)

$$DQ \xrightarrow{h\nu} {}^1DQ^* \xrightarrow{ISC} {}^3DQ^* \quad (1)$$

$$^3DQ^* + DQ(^3DQ^*) \rightarrow 2DQ \quad (2)$$

The change in solvent property with the addition of IL was further examined by comparing the observed pseudo-first-order decay rate constants (k_{obs}) of ^{3}DQ* in solutions with different volume fractions of [bmim][PF_6]. The k_{obs} values were calculated from the decay of absorption at 480 nm. As shown in Figure 2, one critical point (turnover) was observed at $V_{IL} = 0.3$. Before the critical point, the decay rate constant increases obviously with increasing V_{IL}; after the critical point, however, the decay rate constant decreases rapidly with increasing V_{IL}. In all cases, the quantum yield of ^{3}DQ* does not obviously change with increasing V_{IL} because the absorption of ^{3}DQ* remains almost constant.

3. 2. Photoinduced Electron Transfer between ^{3}DQ* and TMPD in IL/MeCN Solutions. There has been some work focusing on the photoinduced electron-transfer (PET) process in ionic liquids.[20,21,24−26] The excited triplet state of the compound has a higher electron affinity than its ground state, and *N*,*N*,*N*′,*N*′-tetramethyl-*p*-phenylenediamine (TMPD) is widely used as an electron donor.[41] Here, we investigated the electron-

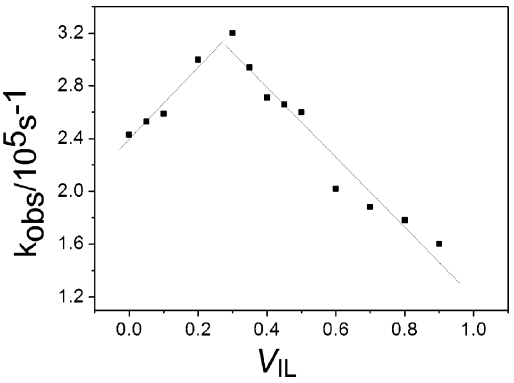

Figure 2. Dependence of the ^{3}DQ* decay rate constant (k_{obs}) at 480 nm on V_{IL} in mixed solutions. ($V_{IL} = 0.3$ corresponds to a mole fraction of about 0.1.)

transfer process of ^{3}DQ* using TMPD as an electron donor in the IL/MeCN solutions.

In the presence of TMPD, new absorption bands appear at longer times (after 1 μs), indicating the formation of new transient species via the reaction of ^{3}DQ* with TMPD since TMPD itself cannot be excited at 355 nm (Figure 3). The absorption bands with λ_{max} at 565 and 610 nm can be assigned to the radical cation of TMPD (TMPD$^{\bullet+}$),[41] while the absorption centering at 410 nm is ascribed to the semiquinone radical, DQ$^{\bullet-}$/DQH$^{\bullet}$, since the spectra of DQ$^{\bullet-}$ and DQH$^{\bullet}$ are nearly identical.[39] At 5 μs after the laser pulse, the peaks of TMPD$^{\bullet+}$ reach their maxima, and the band at 480 nm due to ^{3}DQ* disappears completely.

The above results can be interpreted by eqs 3 and 4. The contact ion pair [DQ$^-\cdots$TMPD$^+$] is formed via electron transfer (ET) and then dissociates into solvent-separated ions TMPD$^{\bullet+}$ and DQ$^{\bullet-}$. At the same time, it may return to DQ and TMPD by back electron transfer (BET). DQ$^{\bullet-}$ can be protonated rapidly to DQH$^{\bullet}$ if a hydrogen donor (RH) such as water exists in the solvent.[37] In our case, we think DQ$^{\bullet-}$ mainly contributes to the 410 nm peak because the solvent in our experiment is pure enough.

$$\mathrm{DQ} + \mathrm{TMPD} \underset{\mathrm{BET}}{\overset{h\nu\ \mathrm{ET}}{\rightleftharpoons}} [\mathrm{DQ}^- \cdots \mathrm{TMPD}^+] \rightleftarrows \mathrm{DQ}^{\bullet-} + \mathrm{TMPD}^{\bullet+} \quad (3)$$

$$\mathrm{DQ}^{\bullet-} + \mathrm{H}^+ \rightleftarrows \mathrm{DQH}^{\bullet} \quad (4)$$

To confirm our speculation, the observed first-order growth rate of TMPD$^{\bullet+}$ at 565 nm is plotted as a function of TMPD concentration, [TMPD]. Since the plot shows a straight line (inset of Figure 3a), the bimolecular rate constant for the reaction of TMPD with ^{3}DQ* is determined to be 7.2×10^9 mol^{-1} dm^3 s^{-1}.

The same investigations were further done in IL/MeCN mixed solutions to compare the reaction of ^{3}DQ* with TMPD in the mixed solutions with different V_{IL} under identical conditions. Figure 4 shows the transient absorption spectra recorded after 355 nm laser excitation in the IL/MeCN (V_{IL}=0.8) solution under N_2 purging. It is seen that the transient absorption spectra in the N_2-saturated IL/MeCN solution are different from that in neat MeCN. At 5 μs after the laser pulse, the peaks due to TMPD$^{\bullet+}$ are not obviously observed, and the band at 460 nm has not completely disappeared. This means that the electron-transfer process is much slower in IL/MeCN and the transient species have longer lifetimes.

To further understand the effect of IL on the electron-transfer process, we chose to analyze the kinetics of the band at 565 nm. Figure 5 shows the dependence of the observed growth rate constant (k_{gr}) of TMPD$^{\bullet+}$ on V_{IL}. It shows a special change with V_{IL}. When IL is dilute ($V_{IL} < 0.10$), the k_{gr} at 565 nm decreases sharply with increasing V_{IL}; when $0.1 < V_{IL} < 0.3$, the k_{gr} increases with increasing V_{IL}; and when $V_{IL} > 0.3$, the k_{gr} decreases again with increasing V_{IL}. In all cases, the values of k_{gr} in the mixtures are always smaller than those in neat MeCN.

The quantum yields of transient species can be obtained based on the formula $\Phi = n/m$, where n is the number of transient products and m is the number of photons absorbed by the reactant.[20] Here, n is equal to cN (N is Avogadro's constant; c is the concentration of the transient product). As we know, $\Delta OD_t = c_t \epsilon l$, where ΔOD_t is the transient absorption, c_t is the concentration of the transient product at time t, ϵ is the molar absorption coefficient, and l is the optical path length. Therefore $\Phi = N\Delta OD_{max}/\epsilon l m$, where ΔOD_{max} is the maximal transient absorption, indicating that the quantum yield of the same species is proportional to ΔOD_{max}. If we mark the quantum yield and the maximal transient absorption in MeCN as Φ_0 and ΔOD_0, then the relative quantum yield in the mixtures can be estimated through $\Phi/\Phi_0 = \Delta OD_{max}/\Delta OD_0$. The relative quantum yields of TMPD$^{\bullet+}$ are shown in Table 1. When the V_{IL} is large enough, the quantum yield of TMPD$^{\bullet+}$ is obviously lower than that in MeCN because the absorption of TMPD$^{\bullet+}$ is very low.

3.3. Fluorescence of the IL/MeCN Mixture. The fluorescence behavior of neat [bmim][PF_6] has been investigated previously by Samanta and co-workers.[7] These authors observed an excitation-wavelength-dependent shift of the emission maximum of [bmim][PF_6] at room temperature, and this may be a general phenomenon for all imidazolium ionic liquids.[15−17] It is suggested that various associated forms of imidazolium cations exist and that the short wavelength emission is due to the monomeric form of the imidazolium cation, while the long wavelength emission is due to its associated forms. It is our interest to investigate the fluorescence behavior of the IL/MeCN binary solutions in different volume ratios in order to understand the local structure character of the mixed solutions and correlate this observation with the reaction kinetic behavior revealed by laser photolysis. We found that the fluorescence behavior of the [bmim][PF_6]/MeCN mixed solutions is similar to that of neat [bmim][PF_6], that is, the emission maximum is strongly dependent on the excitation wavelength. In this work, mixed IL/MeCN solutions in different volume ratios were excited at 280 and 360 nm to investigate the change in ratio of monomeric to associated forms of bmim$^+$ with V_{IL}. As shown Figure 6I−IV, when excited at 280 nm, the emission peaks are at shorter wavelength, and the fluorescence intensity increases sharply with an increasing V_{IL} at $V_{IL} < 0.4$ and then decreases gradually with increasing V_{IL}. However, when excited at 360 nm, the emission peaks appear at a longer wavelength, and the fluorescence intensity increases regularly with the increasing of V_{IL}. It is also seen that when exited at 280 nm, the emission peak shifts slightly to longer wavelengths with increasing V_{IL}, but no shift is observed for the excitation at 360 nm. This indicates that the IL/MeCN mixed solutions are inhomogeneous.

Analogous to the conclusion of Samanta and co-workers for the neat [bmim][PF_6], we assign the fluorescence emission by excitation at 360 nm to the associated forms of imidazolium cations and the fluorescence emission by excitation at 280 nm to the monomeric form of the cations. The slight red shift of the emission peak with V_{IL} for the excitation of IL/MeCN mixed solutions at 280 nm indicates that the contribution of the associated forms of bmim$^+$ in this case is minor while the role

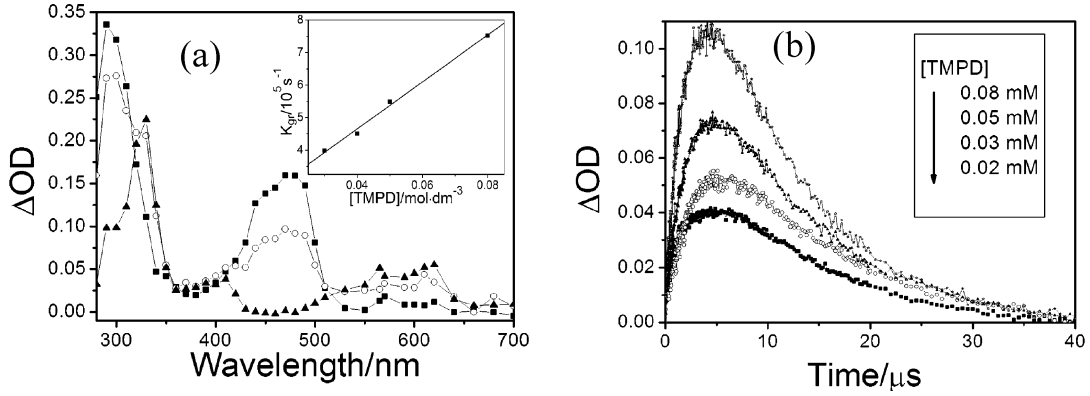

Figure 3. (a) Transient absorption spectra recorded at (■) 0.1, (○) 1, and (▲) 5 μs after 355 nm excitation of the N_2-saturated neat MeCN containing 1×10^{-4} mol·dm^{-3} DQ and 1×10^{-4} mol·dm^{-3} TMPD. Inset: The first-order growth rate of TMPD$^{\bullet+}$ at 565 nm is plotted as a function of TMPD concentration. (b) Time profiles observed at 565 nm for TMPD$^{\bullet+}$.

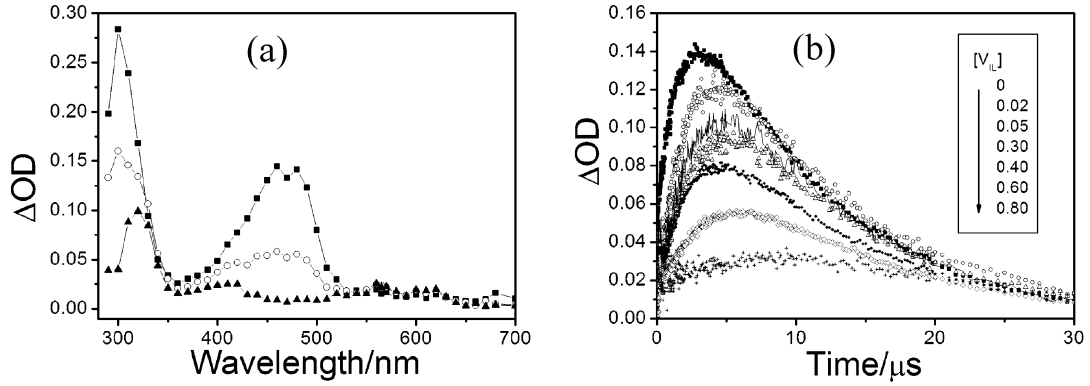

Figure 4. (a) Transient absorption spectra recorded at (■) 1, (○) 5, and (▲) 10 μs after 355 nm excitation for a N_2-saturated IL/MeCN solution ($V_{IL} = 0.8$) containing 1×10^{-4} mol·dm^{-3} DQ and 1×10^{-4} mol·dm^{-3} TMPD. (b) Time profiles of TMPD$^{\bullet+}$ observed at 565 nm for IL/MeCN solutions with different V_{IL} values.

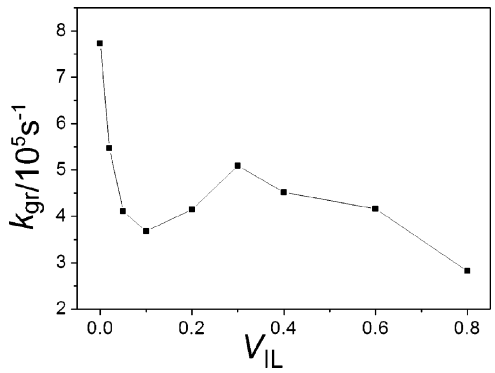

Figure 5. Dependence of the observed growth rate constant (k_{gr}) of TMPD$^{\bullet+}$ on the volume fraction of [bmim][PF_6]. ($V_{IL} = 0.1$ corresponds to a mole fraction of about 0.027.)

TABLE 1: The Relative Quantum Yields of TMPD$^{\bullet+}$ Estimated through $\Phi/\Phi_0 = \Delta OD_{max}/\Delta OD_0$

V_{IL}	0	0.02	0.05	0.1	0.2	0.3	0.4	0.6	0.8
Φ/Φ_0	1	0.73	0.60	0.48	0.52	0.70	0.73	0.38	0.19

of monomeric bmim$^+$ is dominant. With increasing of the V_{IL}, the ratio of monomeric bmim$^+$ to its associated forms will be changed, and this change may be illustrated by the V_{IL} dependence of the emission intensity. If we ignore the contribution of the associated bmim$^+$ to the fluorescence for the excitation at 280 nm, the ratio of the fluorescence peak intensity, I_{280}/I_{360}, can be simply taken as the ratio of monomer to associated forms for [bmim][PF_6]. As shown in Figure 6IV, the I_{280}/I_{360} ratio decreases rapidly and nonlinearly with increasing of the V_{IL}. The monomeric form is dominant at $V_{IL} < 0.1$, and the associated forms become dominant at $V_{IL} > 0.3$. This indicates that the degree of self-aggregation of bmim$^+$ increases significantly with V_{IL}. Therefore, for the reactions involved by bmim$^+$, the overall reaction rate constants will be complex due to the association of bmim$^+$ at higher V_{IL}. This provides a good explanation for our observed turnover of the decay rate constant of DQ* (k_{obs}) and the special change of the observed growth rate constant (k_{gr}) of TMPD$^{\bullet+}$ with increasing V_{IL} for the IL/MeCN mixed solutions.

3.4. Thermodynamic Properties of the Mixtures by Molecular Dynamics Simulation. Since it is difficult to directly measure some properties of ionic liquids such as the enthalpy of vaporization for their low volatility, we present some properties of the IL/MeCN mixtures here by molecular dynamics simulation. The calculations were performed in the *NPT* ensemble at $T = 300$ K and $P = 0.1$ MPa. After the system had achieved equilibrium, simulation runs of 2 ns were carried out, and the data were collected during the last 100 ps. The simulation results are shown in Table 2. The densities of neat [bmim][PF_6] and MeCN are in good agreement with the experiment,[42,43] with a difference of less than 4%.

The cohesion of the particle in the liquid phase can be measured by the enthalpy of vaporization (ΔH^{vap}) of the liquid. ΔH^{vap} values of the mixture are calculated by the method depicted in many literature studies.[44,45] For pure IL, the simulated ΔH^{vap} value is 184.35 kJ mol^{-1}, in good agreement with the value of 189 kJ mol^{-1} estimated from the bimolecular rate constant experiments by Swiderski et al.[46]

The nonideality of a mixture can be depicted by the excess properties. Figure 7 shows the excess molar volume V^E as a function of the mole fraction of IL, x_1. As is seen, V^E is negative

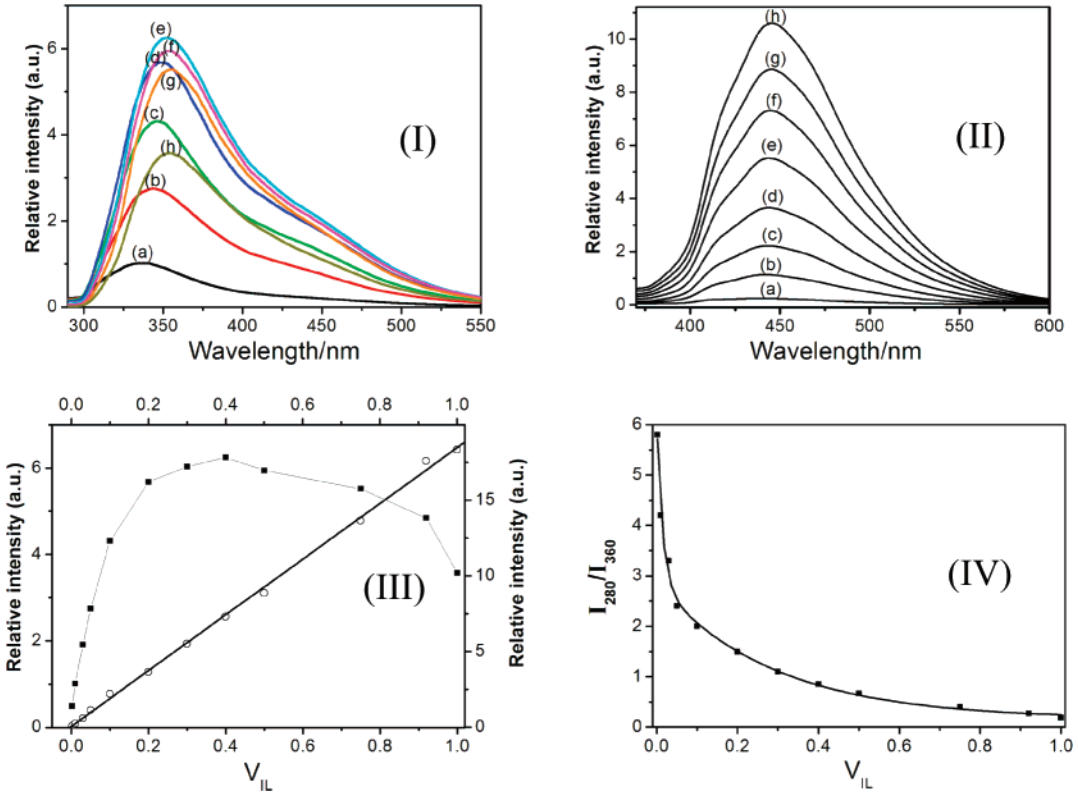

Figure 6. Fluorescence spectra of the mixture of [bmim][PF_6] and MeCN. (I) Excitation wavelength of $\lambda_{exc} = 280$ nm. The values of the volume fraction of [bmim][PF_6] V_{IL} are (a) 0.01, (b) 0.05, (c) 0.1, (d) 0.2, (e) 0.4, (f) 0.5, (g) 0.75, and (h) 1. (II) Excitation wavelength of $\lambda_{exc} = 360$ nm; the V_{IL} values are (a) 0.01, (b) 0.05, (c) 0.1, (d) 0.2, (e) 0.3, (f) 0.4, (g) 0.5, and (h) 0.6. (III) Dependences of the maximum of the fluorescence intensity on V_{IL} (■) at $\lambda_{exc} = 280$ (○) and 360 nm. (IV) Dependence of the fluorescence intensity I_{280}/I_{360} on V_{IL}.

TABLE 2: System Sizes of [bmim][PF_6] (1) + MeCN (2) and Some Simulation Results for the Mixtures at $T = 300$ K and $P = 0.1$ MPa[a]

N_1	N_2	x_1	$\sim V_{IL}$	ρ/g cm^{-3}	ΔH^{vap}/kJ mol^{-1}
0	216	0	0	0.746	33.69
7	249	0.027	0.1	0.821	39.10
15	241	0.059	0.2	0.893	44.73
25	231	0.098	0.3	0.956	50.62
37	219	0.145	0.4	1.007	57.66
43	213	0.168	0.5	1.036	61.14
71	185	0.277	0.6	1.121	87.75
95	161	0.371	0.7	1.171	92.04
129	127	0.504	0.8	1.218	110.92
178	78	0.695	0.9	1.280	140.14
128	0	1.0	1.0	1.334	184.35

[a] N_1 is the particle number of [bmim][PF_6], and N_2 is the particle number of MeCN; x_1 is the mole fraction, and V_{IL} is the approximate volume fraction of [bmim][PF_6] in the mixture; ρ is the density of the mixture; ΔH^{vap} is enthalpy of vaporization of the system.

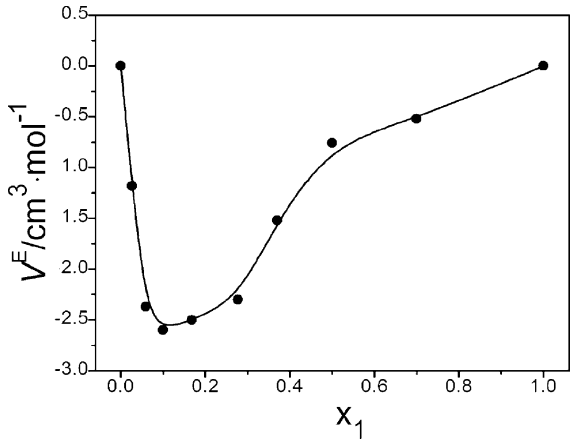

Figure 7. Excess molar volume V^E of the mixture [bmim][PF_6]/MeCN as a function of the mole fraction of [bmim][PF_6], x_1, at $T = 300$ K and $P = 0.1$ MPa.

over the whole range of composition, and it decreases very rapidly at low mole fractions of IL, which is similar to the experimental data.[47] The measured negative V^E values indicate that the interaction in the mixture is larger than that in the pure component.

In addition, we investigated the change of the enthalpy of the mixture. According to the literature,[44] in a liquid phase, the excess molar enthalpy H^E equals approximately the excess molar intermolecular energy U^E. As is shown in Figure 8, H^E is always negative in all mixtures and shows a slow change at $x_1 = 0.1-0.4$.

3.5. Mechanism. Dupont[6] has proposed that imidazolium ionic liquids are hydrogen-bond polymeric supramolecules based on many experimental studies such as IR and NMR analyses. As for [bmim][PF_6], the network is formed by the C−H···F hydrogen bond, which shows characteristic IR spectra in the region of 3100−3200 cm^{-1} pertaining to the interaction of H of the imidazolium cations with the anions. The introduction of other molecules and macromolecules may cause a disruption of the hydrogen-bond network and, in some cases, generates nanostructures with polar and nonpolar regions. In this ionic "cage", the diffusion of solute must be very slow due to the high viscosity and possible interaction with ions. Recently, by MD simulation, Lopes and Pádua showed that ILs with longer alkyl chains might be separated into two types of regions, nonpolar regions arising from aggregating of the alkyl chains and polar regions arising from charge ordering of the anions and imidazolium rings of the cations. The polar regions are interconnected to form a three-dimensional ionic network permeated by nonpolar regions.[30]

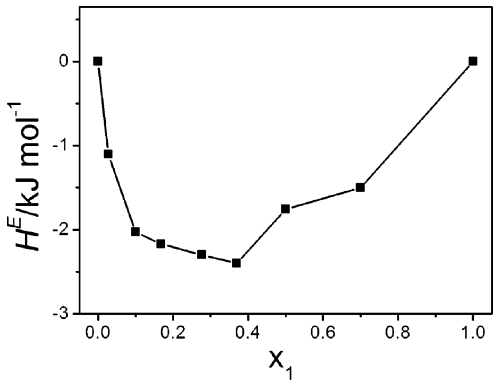

Figure 8. Excess enthalpy of mixing for [bmim][PF_6] (1) + MeCN (2) as a function of the mole fraction of [bmim][PF_6], x_1, at $T = 300$ K and $P = 0.1$ MPa.

The above theories are consistent with our results. The study of fluorescence behavior of the IL/MeCN mixture has proved the transformation of IL from the monomeric form to associated forms. The measured negative V^E and H^E values indicate strong interactions between IL and MeCN, which may destroy the hydrogen-bond network.

The spectral shift of ^{3}DQ* and the critical point of k_{obs} should be due to the changes of the microstructure and properties of the mixtures, as well as the possible strong interaction between DQ and [bmim][PF_6]. According to our results and the theory of Dupont et al.,[6] we propose the model as follows. When the concentration of [bmim][PF_6] is substantially smaller than that of MeCN, the ionic liquid mainly exists in the form of solvent-separated ion pairs. Our fluorescence measurement (Figure 6II) shows that the emission intensity ($\lambda_{exc} = 360$ nm) due to the associated forms of bmim$^+$ is negligible at $V_{IL} = 0.01$. Also, the excess properties rapidly decrease at low x_1, indicating that IL disperses well in MeCN. With increasing V_{IL}, the polarity of the solution increases since [bmim][PF_6] is more polar than acetonitrile.[23] The increase of k_{obs} with V_{IL} before the critical point can be explained by the combination of DQ with [bmim]-[PF_6] and the increase of solvent polarity. After the critical point, a hydrogen-bond network of [bmim][PF_6] is basically formed, and DQ is partly confined in the "cage" of [bmim][PF_6] molecules. This cage effect contributes to the slower molecular diffusion and makes the absorption of the triplet excited states enhanced.[22] Therefore, k_{obs} decreases with a further increasing of [bmim][PF_6] after the critical point.

Previously, we had measured the electrical conductivity of [bmim][PF_6]/MeCN binary mixtures and shown that the maximum conductivity of [bmim][PF_6]/MeCN is 37.9 mS cm^{-1} at V_{IL}=0.32.[27] This value is consistent with the critical point (or turnover) for the k_{obs} indicated in this work. It is considered that the V_{IL} dependence of k_{obs} may be due to many factors, for example, concentration, polarity, and local structure transformation.

The bimolecular PET reaction rate (k_{et}) can be effected by many factors. It is well-known that rates of most PET reactions are governed by the relationship proposed by Marcus et al.[48] Marcus theory was widely applied to interpret the electron-transfer reaction in conventional solvents.

In a PET process, it is more appropriate that the activation barrier (ΔG^+) is predicted by the Rehm−Weller equation[49]

$$\Delta G^+ = \frac{\Delta G^0}{2} + \left[\left(\frac{\Delta G^0}{2}\right)^2 + \left(\frac{\lambda}{2}\right)^2\right]^{1/2} \quad (5)$$

where the change in free energy ΔG^0 is the thermodynamic driving force and λ represents the reorganization energy, which can be summarized by the following equation

$$\lambda = \lambda_s + \lambda_i \quad (6)$$

where λ_i is the intramolecular (inner-sphere) contribution to the total reorganization energy and λ_s is the solvent (outer-sphere) contribution.

Generally, the λ_s term is the predominant contributor to λ. Therefore, it can be concluded that the value of λ depends on solvent polarity. It has been predicted that the λ_s value is 10−20 kJ mol^{-1} higher in ILs than that in MeCN by Shim and Kim.[50] A small change of ΔG^0 for the pyrene-*N*,*N*-dimethylaniline system was estimated in some ILs compared to that in MeCN by Samanta et al.[20] If this small change of ΔG^0 is neglected, a general trend of decreasing k_{et} with increasing λ is expected. From this point of view, the solvent reorganization energy λ_s will increase, and then, k_{et} decreases with increasing V_{IL} in the mixture of [bmim][PF_6]/MeCN. In fact, the k_{gr} of TMPD$^{\bullet+}$ in our experiment shows a special change with V_{IL}, which is different from the dependence of the theoretic value (k_{et}) on V_{IL}.

Some workers have recently made efforts to apply Marcus theory to redox processes in ionic liquids by classical molecular simulations.[51] They also concluded that although Marcus theory could apply to ionic liquids with small cations, the increased heterogeneity and slower dynamics found in ionic liquids with larger cations suggest that the redox process in some ionic liquids may be more complex. This is in support of our conclusion. The difference between the trend of k_{gr} and k_{et} perhaps arises from other factors such as the local structure transformation.

As for the effects of the ionic liquid on the photoinduced electron transfer between ^{3}DQ* and TMPD, we should take salt and cage effects into account. When IL is very dilute ($V_{IL} <$ 0.1), ionic liquid molecules mainly exist in the form of solvent-separated ion pairs; therefore, ionic strength increases with the concentration of IL, which will affect the rate constant due to the salt effect.[52,53] When the concentration of IL increases, contact ion pairs of IL are formed, and the salt effect on the rate constant becomes less important. At the same time, the solvent reorganization energy increases with increasing solvent polarity. When the concentration of IL is further increased, a hydrogen-bond network of [bmim][PF_6] is formed. Therefore, the viscosity of the solution increases, and the diffusion rates of the solutes are decreased. The probability of the contact ion pairs [DQ$^-$···TMPD$^+$] escaping from the cage decreases. The cage effect makes the lifetime of ion pairs of [DQ$^-$···TMPD$^+$] longer and results in higher efficiency of the back electron transfer. Consequently, slow diffusion and a lower escape rate are responsible for the low efficiency of the solvent-separated photoinduced electron-transfer products. The cause of a special change of k_{gr} might be the combined result of many factors, including the local structure and the reorganization energy of the solvent and salt and cage effects.

4. Conclusion

A systematic study of the effects of [bmim][PF_6] on transient absorption spectra and photoinduced the electron-transfer process in MeCN has been undertaken by laser photolysis. Our results reveal that the IL/MeCN mixed solutions possess some particular properties differing from those of the neat IL or organic solvent. Along with the change of the volume ratio of

IL/MeCN, a spectral blue shift of ^{3}DQ* was observed, and the decay rate constant (k_{obs}) of ^{3}DQ* changed significantly. According to PET theory, it is suggested that k_{et} will decrease with increasing V_{IL} in the mixture of [bmim][PF_6]/MeCN, being somewhat different from the trend of the k_{gr} of $TMPD^{\bullet+}$ in our experiment. Our results indicate that the effects of ionic liquid on the PET reaction kinetics between ^{3}DQ* and TMPD at various V_{IL} values are very complicated. We associate the effects with the local structure as well as the solvent property of the mixture of [bmim][PF_6]/MeCN, supported by the fluorescence measurement and molecular dynamics simulation.

Acknowledgment. This work was financially supported by the National Natural Science Foundation of China (No. 20673137).

Supporting Information Available: Dependence of some rate constants on mole fraction of [bmim][PF_6], snapshot of ion pairs of [bmim][PF_6] extracted from the mixtures, IR spectra of [bmim][PF_6], and fluorescence spectra of the mixture of [bmim][PF_6]/MeCN at V_{IL}=0.1, 1. This material is available free of charge via the Internet at http://pubs.acs.org.

References and Notes

(1) Welton, T. *Chem. Rev.* **1999**, *99*, 2071.
(2) Rogers, R. D.; Seddon, K. R. *Science* **2003**, *302*, 792.
(3) Gutowski, K. E.; Broker, G. A. *J. Am. Chem. Soc.* **2003**, *125*, 6632.
(4) Dupont, J.; de Souza, R. F.; Suarez, P. A. Z. *Chem. Rev.* **2002**, *102*, 3667.
(5) Wu, G. Z.; Liu, Y. D.; Long, D. W. *Macromol. Rapid Commun.* **2005**, *26*, 57.
(6) Dupont, J. *J. Braz. Chem. Soc.* **2004**, *15*, 341.
(7) Paul, A.; Mandal, P.; Samanta, A. *Chem. Phys. Lett.* **2005**, *402*, 375.
(8) Talaty, E. R.; Raja, S.; Storhaug, V. J.; Dolle, A.; Carper, W. R. *J. Phys. Chem. B* **2004**, *108*, 13177.
(9) Liu, Y. D.; Zhang, Y.; Wu, G. Z.; Hu, J. *J. Am. Chem. Soc.* **2006**, *128*, 7456.
(10) Marcinek, A.; Zielonka, J.; Gebicki, J. *J. Phys. Chem. A* **2001**, *105*, 9305.
(11) Wishart, J. F.; Neta, P. *J. Phys. Chem. B* **2003**, 107, 7261.
(12) Baker, S. N.; Baker, G. A.; Kane, M. A.; Bright, F. V. *J. Phys. Chem. B* **2001**, *105*, 9663.
(13) Karmakar, R.; Samanta, A. R. *Chem. Phys. Lett.* **2003**, *376*, 638.
(14) Grodkowski, J.; Neta, P. *J. Phys. Chem. A* **2002**, *106*, 5468.
(15) Karmakar, R.; Samanta, A. R. *J. Phys. Chem. A* **2002**, *106*, 6670.
(16) Karmakar, R.; Samanta, A. *J. Phys. Chem. A* **2003**, *107*, 7340.
(17) Samanta, A. *J. Phys. Chem. B* **2006**, *110*, 13704.
(18) Ito, N.; Arzhantsev, S.; Maroncelli, M. *Chem. Phys. Lett.* **2004**, *396*, 83.
(19) Ingram, J. A.; Moog, R. S.; Ito, N.; Biswas, R.; Maroncelli, M. *J. Phys. Chem. B* **2003**, *107*, 5926.
(20) Paul, A.; Samanta, A. *J. Phys. Chem. B* **2007**, *111*, 1957.
(21) Marquis, S.; Ferrer, B.; Alvaro, M.; García, H.; Roth, H. D. *J. Phys. Chem. B* **2006**, *110*, 14956.
(22) Alvaro, M.; García, H. *Chem. Phys. Lett.* **2002**, *362*, 435.
(23) Gordon, C. M.; McLean, A. J. *Chem. Commun.* **2000**, 1395.
(24) Katoh, R.; Yoshida, Y.; Katsumura, Y.; Takahashi, K. *J. Phys. Chem. B* **2007**, *111*, 4770.
(25) Brands, H.; Chandrasekhar, N.; Unterreiner, A. N. *J. Phys. Chem. B* **2007**, *111*, 4830.
(26) Vieira, R. C.; Falvey, D. E. *J. Phys. Chem. B* **2007**, *111*, 5023.
(27) Zhu, G. L.; Xu, J. J.; Wu, G. Z.; Zhu, H. P.; Long, D. W.; Chen, S. M.; Yao, S. D. *Int. J. Mol. Sci.* **2006**, *7*, 590.
(28) Vila, J.; Ginés, P.; Rilo, E.; Cabeza, O.; Varela, L. M. *Fluid Phase Equilib.* **2006**, *247*, 32.
(29) Jarosik, A.; Krajewski, S. R.; Lewandowski, A.; Radzimski, P. *J. Mol. Liq.* **2006**, *123*, 43.
(30) Lopes, J. N. A. C.; Pádua, A. A. H. *J. Phys. Chem. B* **2006**, *110*, 3330.
(31) Zuo, Z. H.; Yao, S. D.; Luo, J.; Wang, W. F.; Zhang, J. S.; Lin, N. Y. *J. Photochem. Photobiol., B* **1992**, *15*, 215.
(32) Lopes, J. N. A. C.; Deschamps, J.; Pádua, A. A. H. *J. Phys. Chem. B* **2004**, *108*, 2038.
(33) (a) Jorgensen, W. L.; Maxwell, D. S.; Tirado-Rives, J. *J. Am. Chem. Soc.* **1996**, *118*, 11225. (b) Kaminski, G.; Jorgensen, W. L. *J. Phys. Chem.* **1996**, *100*, 18010.
(34) Borodin, O.; Smith, G. D.; Jaffe, R. L. *J. Comput. Chem.* **2001**, *22*, 641.
(35) Grabuleda, X.; Jaime, C.; Kollman, P. A. *J. Comput. Chem.* **2000**, *21*, 901.
(36) Lindahl, E.; Hess, B.; van der Spoel, D. *J. Mol. Model.* **2001**, *7*, 306.
(37) Scheerer, R.; Grätzel, M. *J. Am. Chem. Soc.* **1977**, *99*, 865.
(38) Scaiano, J. C.; Neta, P. *J. Am. Chem. Soc.* **1980**, *102*, 1608.
(39) Görner, H. *Photochem. Photobiol.* **2003**, *78*, 440.
(40) Muldoon, M. J.; McLean, A. J.; Gordon, C. M.; Dunkin, I. R. *Chem. Commun.* **2001**, 2364.
(41) Lu, C. Y.; Liu, Y. Y. *Biochim. Biophys. Acta* **2002**, *1571*, 71.
(42) Margulis, C. J.; Stern, H. A.; Berne, B. J. *J. Phys. Chem. B* **2002**, *106*, 12017.
(43) Gallant, R. W. *Hydrocarbon Process.* **1969**, *48*, 135.
(44) (a) Liu, Z. P.; Huang, S. P.; Wang, W. C. *J. Phys. Chem. B* **2004**, *108*, 12978. (b) Wu, X. P.; Liu, Z. P.; Huang, S. P.; Wang, W. C. *Phys. Chem. Chem. Phys.* **2005**, *7*, 2771.
(45) Micaelo, N. M.; Baptista, A. M.; Soares, C. M. *J. Phys. Chem. B* **2006**, *110*, 14444.
(46) Swiderski, K.; McLean, A.; Gordon, C. M.; Vaughan, D. H. *Chem. Commun.* **2004**, 2178.
(47) (a) Zafarani-Moattar, M. T.; Shekaari, H. *J. Chem. Eng. Data* **2005**, *50*, 1694. (b) Zafarani-Moattar, M. T.; Shekaari, H. *J. Chem. Thermodyn.* **2006**, *38*, 1377.
(48) (a) Marcus, R. A. *J. Chem. Phys.* **1956**, *24*, 966. (b) Marcus, R. A. *Annu. Rev. Phys. Chem.* **1964**, *15*, 155. (c) Marcus, R. A. *J. Phys. Chem.* **1968**, *72*, 891. (d) Marcus, R. A. *Rev. Mod. Phys.* **1993**, *65*, 599.
(49) (a) Rehm, D.; Weller, A. *Ber. Bunsen-Ges. Phys. Chem.* **1969**, 73834. (b) Rehm, D.; Weller, A. *Isr. J. Chem.* **1970**, *8*, 259.
(50) Shim, Y.; Kim, H. J. *J. Phys. Chem. B* **2007**, *111*, 4510.
(51) (a) Lynden-Bell, R. M. *J. Phys. Chem. B* **2007**, *111*, 10800. (b) Lynden-Bell, R. M. *Electrochem. Commun.* **2007**, *9*, 1857.
(52) Mac, M.; Wirz, J. *Photochem. Photobiol. Sci.* **2002**, *1*, 24.
(53) Simon, J. D.; Peters, K. S. *J. Am. Chem. Soc.* **1982**, *104*, 6142.